FERMILAB-CONF-10-577-E

New measurement of the B_s mixing phase at the Tevatron

Franco Bedeschi[a] on behalf of the CDF collaboration

[a]INFN - Sezione di Pisa,
Largo B. Pontecorvo 3, 56127 Pisa, Italy

We report the new measurement of the CP violating parameter β_s at CDF with an integrated luminosity of 5.2 fb^{-1}. This result updates previous measurements of CDF and DØ and is consistent with the Standard Model prediction at the 1 σ level. We also obtain the best single experiment measurements of the B_s lifetime, lifetime difference and of the polarization amplitudes for the decay $B_s \to J/\psi\varphi$.

1. INTRODUCTION

The study of the mixing of neutral B mesons is of particular interest as it is sensitive to new physics beyond the Standard Model (SM). The amplitude for the transition between B and $\bar{B}$ is calculated from "box" diagrams where virtual quarks and W's are exchanged; additional such diagrams containing new particles are possible thus changing the theoretical prediction. The magnitude of this transition amplitude is proportional to the mixing frequency, while its phase (mixing phase) is responsible for CP violation and can be related to the phases of specific elements of the CKM matrix [1]. Both the magnitude and the phase need to be measured in order to constrain, or demonstrate, new physics.

In the case of the B_d the B-factories have done an excellent work in the measurement of both the mixing frequency and the mixing phase, which resulted in a fairly strong constraint on new physics [2] [3].

The situation is much more open in the case of the B_s. Indeed while the mixing frequency has been accurately measured in 2006 by CDF [4] and then confirmed by DØ [5] and found in good agreement with SM predictions, as of last year the combined measurement of the phase by the two Tevatron experiment still had a very large uncertainty. Nonetheless those measurements indicated a discrepancy at the 2.1 σ level with the SM, which has generated much interest from the theorists [6] and, as a consequence, a strong experimental effort to improve the result. The interest has been further increased by the recent related measurement of the B semileptonic asymmetry by the DØ experiment [7], which indicates a 3 σ discrepancy from the SM.

In the following we present the new CDF measurement of the mixing phase, which improves significantly the previous result by doubling the statistics and refining the analysis technique.

2. THEORY AND NOMENCLATURE

The time evolution of the B_s^0 system is described by the equation [1]:

$$i\frac{d}{dt}\begin{pmatrix} |B_s^0> \\ |\bar{B}_s^0> \end{pmatrix} = \mathbf{H}\begin{pmatrix} |B_s^0> \\ |\bar{B}_s^0> \end{pmatrix} \quad (1)$$

with an effective Hamiltonian

$$\mathbf{H} = \begin{pmatrix} M - i\frac{\Gamma}{2} & M_{12} - i\frac{\Gamma_{12}}{2} \\ M_{12}^* - i\frac{\Gamma_{12}^*}{2} & M - i\frac{\Gamma}{2} \end{pmatrix} \quad (2)$$

where M and Γ are the average mass and width of the B_s^0's; M_{12} is the transition amplitude from B_s^0 to $\bar{B}_s^0$ via flavor changing box diagrams and Γ_{12} is a parameter related to the decay to final states which are common to both B_s^0 and $\bar{B}_s^0$.

The mass eigenstates, defined as the eigenvectors of the above matrix, are different from the flavor eigenstates, with a heavy (H) and light (L) mass eigenstate. Matrix elements can be extracted experimentally by measuring a mass and width difference between mass eigenstates:

$$\Delta m_s = M_H - M_L \approx 2|M_{12}| \quad (3)$$

$$\Delta\Gamma_s = \Gamma_L - \Gamma_H \approx 2|\Gamma_{12}| cos\,\phi_s \quad (4)$$

where

$$\phi_s = arg\left(-\frac{M_{12}}{\Gamma_{12}}\right) \quad (5)$$

The SM predicts a very small value for the phase of both M_{12} and Γ_{12} resulting in a tiny value of $\phi_s = 0.004$ [1]. In this notation the semileptonic asymmetry recently measured by DØ is given by:

$$a^s_{sl} = \frac{|\Gamma_{12}|}{|M_{12}|} sin\,\phi_s = \frac{\Delta\Gamma_s}{\Delta m_s} tan\,\phi_s \quad (6)$$

and is therefore expected to be at the 10^{-5} level in the SM.

In the context of the SM it can be shown [1] that (assuming the PDG [8] phase convention for the CKM [9] elements $V_{qq'}$):

$$M_{12} \propto (V^*_{ts}V_{tb})^2 \propto e^{-2i\beta^{SM}_s} \quad (7)$$

where β^{SM}_s is defined in terms of the CKM elements which control the mixing and the decay of B^0_s mesons to specific $b \to c\bar{c}s$ quark transitions:

$$\beta^{SM}_s = arg\left(-\frac{V_{ts}V^*_{tb}}{V_{cs}V^*_{cb}}\right) \quad (8)$$

The presence of new physics can add an additional phase, ϕ^{NP}_s, to M_{12} if new particles are exchanged in the "box" diagrams. The effect is expected to be much smaller in Γ_{12} which is dominated by tree level processes. Therefore a measurement sensitive to $2\beta^{SM}_s$ would measure instead $2\beta_s = 2\beta^{SM}_s - \phi^{NP}_s$, while a measurement sensitive to ϕ^{SM}_s would measure instead $\phi_s = \phi^{SM}_s + \phi^{NP}_s$. The current experimental precision does not allow these small CP-violating phases ϕ^{SM}_s and β^{SM}_s to be resolved, and for a large new physics effect, we can approximate $\phi_s \approx -2\beta_s \approx \phi^{NP}_s$; i.e., a significantly large observed phase would indicate new physics. This approximation is commonly used by Tevatron experiments.

3. THE CDF MEASUREMENT

The final state $J/\psi\varphi$ is common to B_s and $\bar{B}_s$, so it can be reached either directly, as in $B_s \to J/\psi\varphi$, or after mixing, as in $B_s \to \bar{B}_s \to J/\psi\varphi$. These two amplitudes interfere and the combined decay width depends on $2\beta_s$. This dependence however changes sign depending on whether the initial state is a B_s or a $\bar{B}_s$ and on the CP value of the final state. This has two important experimental implications:

- determining the flavor of the initial state, i.e. flavor tagging;
- unfolding the CP-even and CP-odd components of the final state by performing an angular analysis. Indeed the process considered is a decay of a spin 0 to two spin 1 particles; this configuration has several possible orbital angular momenta: $L = 0, 2$, which are CP-even, and $L = 1$, which is CP-odd.

CDF uses a sample of $B_s \to J/\psi\varphi$ decays to measure β_s. In this analysis several improvements have been introduced with respect to previous analyses [10], [11], [12]:

- the data sample has been doubled and the signal selection optimized with a Neural Net (NN);
- the flavor tagging has been completely recalibrated both for the opposite side tagging and the same side tagging;
- the contribution of a scalar component such as $B_s \to J/\psi f_0$ has been fully included into the fit.

In the following we describe in more detail all components of the analysis.

3.1. Signal selection

The data sample corresponds to an integrated luminosity of 5.2 fb^{-1} collected with the di-muon J/ψ trigger [13].

After a loose selection based on track and vertex fit quality and basic kinematical cuts, we use a NN to optimize the candidate selection. The NN is trained using Monte Carlo events for the signal sample and sideband data events in the mass range [5.2,5.3] GeV/c^2 and [5.45, 5.55] GeV/c^2 for the background. The NN makes use of 10 variables: the p_t of the φ and the B_s, the particle ID

likelihoods for each of the kaons and the muons, and the χ^2's for several intermediate vertex fits.

The final cut on the NN value was chosen to minimize the error on the β_s measurement, as determined in several ensembles of simulated data. In figure 1 we show the final signal distribution containing 6,500 signal events with S/N ≈ 1.

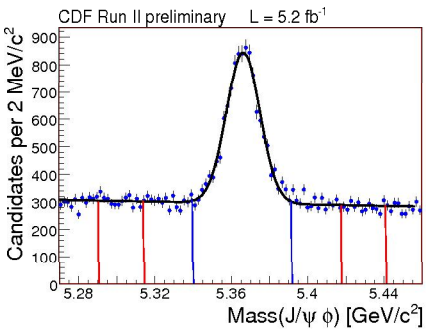

Figure 1. Invariant mass distribution of B_s candidates. The vertical lines indicate the signal and sideband regions.

3.2. Flavor tagging

Different flavor tagging algorithms are used to tag the flavor of the B_s at production. For each event these algorithms output a tag decision as well as a dilution $D = 1 - 2w$, where w is the probability to make the wrong decision. Flavor taggers fall in two main categories: opposite side tagging (OST) and same side tagging (SST).

OST exploits the flavor conservation of strong interactions which ensures that b quarks are always produced in pair with a $\bar{b}$ quark; therefore by tagging the flavor of a b quark in the opposite hemisphere of the signal B_s meson one can infer its flavor at production. CDF uses the charge of electrons (soft electron tagger), muons (soft muon tagger), or jets (jet charge tagger) to determine the flavor of the opposite side b. All these taggers are combined in a single NN to obtain the optimal tagging power.

SST exploits flavor conservation in the fragmentation process of the b quark that forms the B_s as an $s\bar{s}$ pair is needed to make the meson. One strange quark forms the B_s meson, while the other will most likely make a kaon kinematically close to the B_s. The sign of a nearby charged kaon therefore tags the flavor of the B meson. This is by far the most powerful tagging technique at CDF.

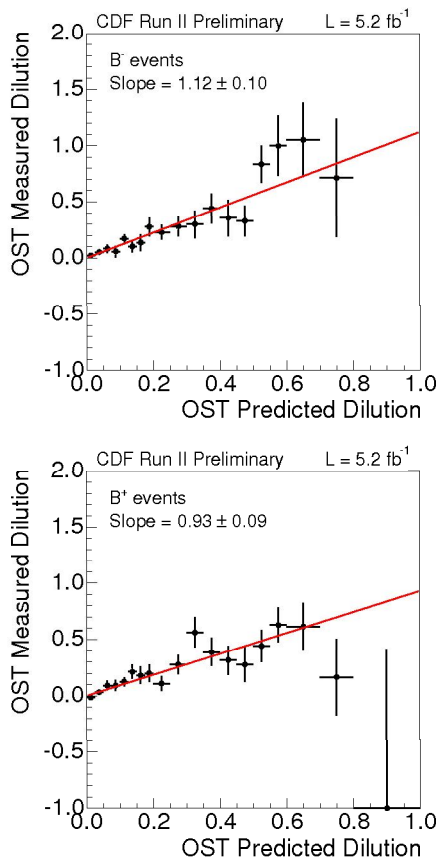

Figure 2. Comparison between predicted and measured dilutions with OST. The slope of the fitted lines determines the scale factor.

The dilution of all flavor taggers is carefully parametrized as a function of many event prop-

erties using Monte Carlo simulations; however we assume that there can be overall scale factors between the simulation and reality that are calibrated directly with data. The uncertainty in their determination is used as an estimate of the associated systematic error.

For OST we can use a flavor specific final state such as $B^{\pm}$ for calibration. In our case we use a sample of 52,000 $B^+ \to J/\psi K^+$ and calibrate independently the negative and positive tags. A comparison of the predicted and measured dilutions is shown in fig. 2 indicating good agreement with scale factors close to 1. The observed tagging efficiency is 94.3 ± 0.3 % and the average predicted dilution on signal is 0.069 ± 0.001.

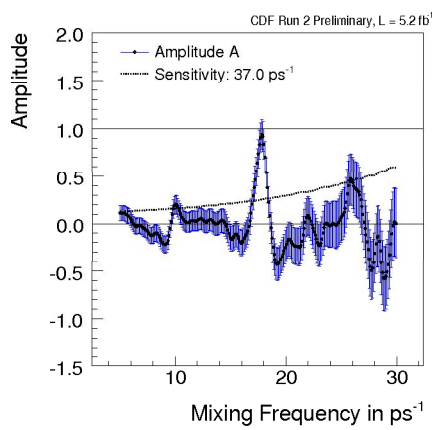

Figure 3. Amplitude scan using SST on a $B_s \to D_s\pi(\pi\pi)$ sample. The amplitude at the resonance defines the scale factor.

The calibration of SST is more difficult because one must use B_s decays into flavor specific final states, such as $D_s^-\pi^+$ or $D_s^-\pi^+\pi^-\pi^+$, and then perform a full B_s mixing analysis [14]. In this case the scale factor is given by the size of the amplitude at the mixing frequency. Using $\sim$ 13,000 $B_s \to D_s^-\pi^+(\pi^-\pi^+)$ events we repeat for the first time since 2006 the B_s mixing analysis and find a perfectly consistent value for the mixing frequency, $\Delta m_s = 17.79 \pm 0.07$ ps^{-1}. The amplitude scan is shown in fig. 3, with a scale factor $A = 0.94 \pm 0.15$(stat) ± 0.13 (syst). We measure a tagging efficiency of 52.2 ± 0.7%, and an average predicted dilution on signal of 0.218 ± 0.003.

3.3. Un-binned maximum likelihood fit

The un-binned maximum likelihood fit is similar to that used previously [10], although an S-wave component has been added to account for possible contamination from $f_0 \to K^+K^-(\pi^+\pi^-)$ or more generally a non-resonant K^+K^- contribution in the φ region [15]. The angular analysis is part of the fitting function and adds three complex polarization amplitudes to the fit parameters. A detailed discussion of the angular analysis can be found in ref. [16].

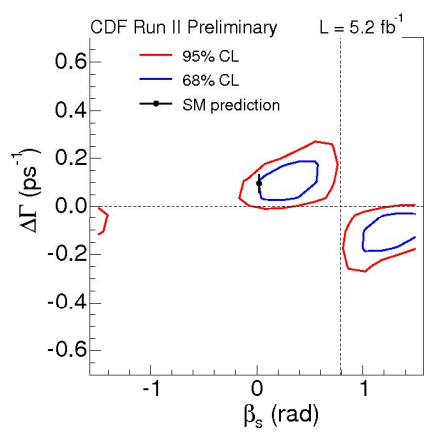

Figure 4. 68% and 95% confidence level contours after full coverage adjustment. The dot indicates the SM prediction.

The likelihood fit is used to extract the parameters of interest, β_s and $\Delta\Gamma_s$, plus additional parameters that include the signal fraction f_s and mass of the B_s, the average B_s lifetime, τ_s, the background lifetime parameters, the mixing frequency Δm_s and flavor tagging efficiencies and scale factors, the magnitude of the polarization amplitudes $|A_0|$, $|A_{\parallel}|$ and $|A_{\perp}|$ and

the relative strong phases $\delta_{\parallel} = arg(A_0^* A_{\parallel})$ and $\delta_{\perp} = arg(A_0^* A_{\perp})$. The inputs to the fit include, for each event, the reconstructed B_s^0 candidate mass m and its uncertainty σ_m, the B_s^0 candidate proper decay time t and its uncertainty σ_t, a vector of 3 angles, $\vec{\rho}$, describing the configuration of the final state, and tag information D and ξ, where D is the event-specific dilution and $\xi = (-1, 0, 1)$ is the tag decision, in which $\xi = 0$ means that no tag is available for that event.

3.4. Results

The fit is extremely complex and the available statistics still rather limited; this makes the distribution of many of the fit parameters, including β_s, highly non-Gaussian. For this reason we prefer to quote the result, shown in fig. 4, in terms of a confidence region in the $\beta_s - \Delta\Gamma$ plane rather then quoting a point value. The contours are fully

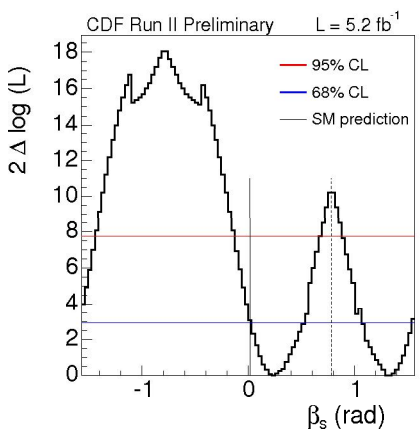

Figure 5. β_s log-likelihood distribution $(log(L_{max}) - log(L(\beta_s)$. Horizontal lines indicate 68% and 95% CL after full coverage adjustment.

corrected for non-Gaussian effects, systematic errors and possible variations of the remaining fit parameters to ensure probability coverage. These corrections degrade the statistical error on β_s by ~20% on average. Fig. 4 also shows the predicted SM point at the boundary of the 68% CL contour. Assuming the SM predictions of β_s and $\Delta\Gamma$, the probability of a deviation as large as the level of the observed data is computed to be 44%, corresponding to 0.8 σ. In fig. 5 we show the 1-dimensional log-likelihood distribution for the parameter β_s. After all corrections we find that $\beta_s \in [0.02,0.52] \cup [1.08,1.55]$ at the 68% CL.

The fit prefers a rather small fraction ($\sim 2\%$) of s-wave contribution in the region $m(K^+K^-) \in [1.009, 1.028]$ GeV/c^2. This fraction is less than 6.7% at the 95% CL. As a consequence we find that the effect of including an s-wave contribution in our fit is negligible at the current level of accuracy.

3.5. Results assuming $\beta_s = 0$

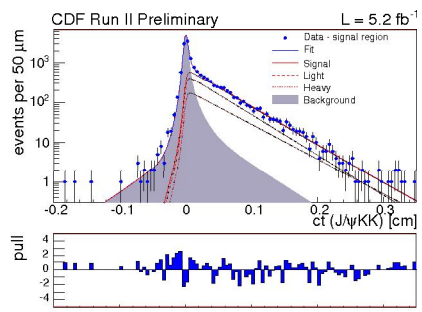

Figure 6. B_s lifetime fit projection.

Assuming for β_s the SM value or 0, which is the same for all practical purposes, makes the likelihood much better behaved at our current level of statistics allowing a point estimate for many of the fit parameters. In particular we can measure the mean B_s lifetime, τ_s, the decay width difference, $\Delta\Gamma_s$, the magnitude of the polarization amplitudes and the strong phase $\delta_{\perp}$. We are still unable to reliably determine a point estimate for $\delta_{\parallel}$ since its central value is close to a symmetry point of the likelihood making the error returned by the fit unreliable. In figure 6

we show the B_s lifetime fit projection which is very well described by the model. The numerical results are shown below:

$$
\begin{aligned}
c\tau_s &= 458.6 \pm 7.6\,(stat.) \pm 3.6\,(syst.)\ \mu m \\
\Delta\Gamma_s &= 0.075 \pm 0.035\,(stat.) \pm 0.01\,(syst.)\ ps^{-1} \\
|A_{\parallel}|^2 &= 0.231 \pm 0.014\,(stat.) \pm 0.015\,(syst.) \\
|A_0|^2 &= 0.524 \pm 0.013\,(stat.) \pm 0.015\,(syst.) \\
\delta_{\perp} &= 2.95 \pm 0.64\,(stat.) \pm 0.07\,(syst.)
\end{aligned}
$$

We note that $|A_{\perp}|^2 = 1 - |A_0|^2 - |A_{\parallel}|^2$. The systematic errors account for uncertainties in the signal and background angular model and efficiencies, the signal and background mass model, the lifetime resolution model, the background lifetime model, the $B^0 \to J/\psi K^{*0}$ cross-feed, the vertex detector alignment, the mass and lifetime resolution distributions and the small remaining fit bias. These results represent the current best single experiment measurements of these quantities.

4. CONCLUSION

This analysis of 5.2 fb^{-1} of CDF data tightens the constraints on β_s and finds the discrepancy with the SM reduced to only about 1 σ. It also provides the current best measurements of the B_s lifetime, $\Delta\Gamma_s$ and the polarization amplitudes for the decay $B_s \to J/\psi\varphi$.

By the end of 2011 we expect to double the statistics and add $\sim$ 30% more data using the track based triggers in addition to the di-muon triggers currently used. Additional decay modes such as $\psi(2S)\varphi$ and $J/\psi f_0$ followed by $f_0 \to \pi^+\pi^-$ can also be used to further increase the signal sample.

By the end of next year the Tevatron will be able to discover or exclude new physics by improving its exclusion of a wide range of β_s parameter space. The race is on with LHCb that has had a very good start-up and is on paper very competitive on this measurement already by the end of next year if LHC delivers the promised luminosity with appropriate beam conditions.

In any case the stage is set for an exciting new year in the study of CP violation in the B_s sector.

REFERENCES

1. A. Lenz and U. Nierste, J. High Energy Physics 06, (2007) 072; arXiV:hep-ph/0612167.
2. M. Bona *et al.* [UTfit Collaboration], JHEP 0507, (2005) 028; M. Bona *et al.* [UTfit Collaboration], JHEP 0610, (2006) 081.
3. J. Charles *et al.* [CKMfitter Group], Eur. Phys. J. C 41, (2005) 1.
4. CDF Collaboration, Phys. Rev. Lett. 97, 242003 (2006).
5. DØ Collaboration, http://www-d0.fnal.gov/Run2Physics/WWW/results/prelim/B/B51/B51.pdf
6. M. Bona *et al.*, arXiv:0803.0659v2 [hep-ph].
7. DØ Collaboration, Fermilab-PUB-10/114-E.
8. K. Nakamura *et al.* (Particle Data Group), J. Phys. G 37, 075021 (2010).
9. M. Kobayashi and T. Maskawa, Prog. Theor. Phys. 49, (1973) 652.
10. CDF Collaboration, Phys. Rev. Lett. 100, 161802 (2008); CDF Public Note 9458, August 7, 2008.
11. DØ Collaboration, Phys. Rev. Lett. 101, 241801 (2008).
12. CDF/DØ Collaborations, http://tevbwg.fnal.gov/results/Summer2009_betas/D0Note5928_CDFNote9787.pdf
13. CDF Collaboration, Phys. Rev. D71, 032001 (2005).
14. CDF Public Note 10108, March 16, 2010.
15. S. Stone and L. Zhang, Phys. Rev. D79, 074024 (2009); Y. Xie, P. Clarke, G. Cowan, and F. Muheim, JHEP 09, 074 (2009).
16. A. S. Dighe *et al.*, Physics Letters B369 (1996) 144-150.